Mineral processing &
Extractive metallurgy

Extract from
Transactions/Section C of the Institution
of Mining and Metallurgy

Volume 77 1968

A three-dimensional diagram for the silver–oxygen system

E. H. Baker and M. I. Talukdar

Automatic control of a concentric cylinders type viscometer

F. A. Garner B.Sc., A.M.I.M.M.
Lecturer, Department of Minerals Engineering, University of Birmingham, Birmingham
M. G. Burcher B.Sc., Stud.I.M.M.
Research Student, Department of Minerals Engineering, University of Birmingham, Birmingham

669.012.1–523:532.137

The measurement of viscosity of liquid slags and metals at high temperatures involves the solution of difficult practical problems. The device described here facilitates the production of continuous viscosity–temperature curves without the operator's intervention, since control and recording are automatic. The control set-up is both simple and inexpensive, and is being used in the Department of Minerals Engineering at the University of Birmingham on slag viscosity problems, but it may be applied whenever the electromagnetically balanced concentric cylinders viscometer is in use.

The viscometer has been constructed in a way that is generally similar to those of Bockris and Lowe,[1] Roberts,[2] Jones[3] and Higgins and Jones.[4] It is of the concentric cylinders type in which the lower cylinder, containing the slag, is rotated when a viscous torque is exerted on a spindle suspended in the melt. A coil attached to the top of the spindle is situated between the poles of a magnet, and a current is passed through this coil until it is of such a magnitude that the electromagnetic torque exactly opposes the viscous torque. It is usual to judge the position of balance by means of a light beam–mirror arrangement. A mirror on the coil reflects a light beam, and the position of the reflected beam on a scale is observed. The operator regulates the current by means of a resistance box. In the present instrument the scale is replaced by a block housing two photocells, the zero point being midway between the two cells. When the light beam deviates from the zero position one cell is illuminated, and the amplified signal from the cell triggers a relay. The relay starts a small, low-speed motor which drives a variable potentiometer in the viscometer coil circuit. The current to the coil is increased or decreased, depending on which photocell is illuminated, and the coil is returned to the zero position. The magnitude of the current is measured by means of a potential divider in the coil circuit and a millivolt chart recorder. A block diagram of the system is given in Fig. 1, and the circuit diagrams are shown in Figs. 2 and 3.

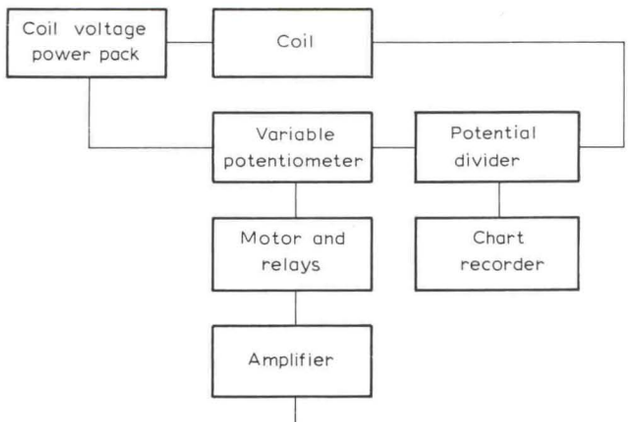

Fig. 1 Block diagram of system

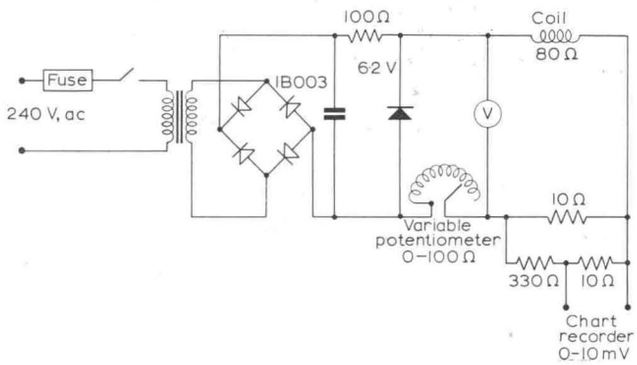

Fig. 2 Coil circuit: this circuit supplies the variable current to the coil by means of a constant voltage source and a variable potentiometer

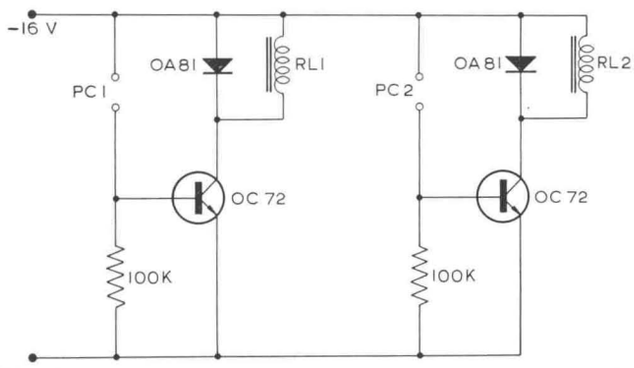

Fig. 3 Detector and amplifier circuit: when photocells PC1 or PC2 are illuminated the amplified signal closes relay RL1 or relay RL2, which starts the potentiometer drive motor

If the viscometer furnace is placed under the control of a programme controller operating at a very slow rate of change, and the furnace and melt temperatures are also monitored by the chart recorder, it is possible to obtain results for viscosity–temperature over a range of temperatures. The changes in dimensions of the apparatus between 1200 and 1400°C (typical copper reverberatory slag temperatures) are small, and their effect on the viscosity measurement is less than the uncertainty in temperature measurement at these temperatures, but the data may be corrected for dimensional changes in the same way as viscosity data obtained by manual control.

The advantages obtained by using automatic control of coil current are that continuous curves of viscosity–

temperature are obtained, and long experimental runs may be made with no operator in attendance. The rate of data collection is improved, and curves may be plotted more fully than was the case with manual control. Reproducibility is at least as good as it is under manual control, and errors introduced by the controller are extremely small compared with errors in the measurement of other parameters.

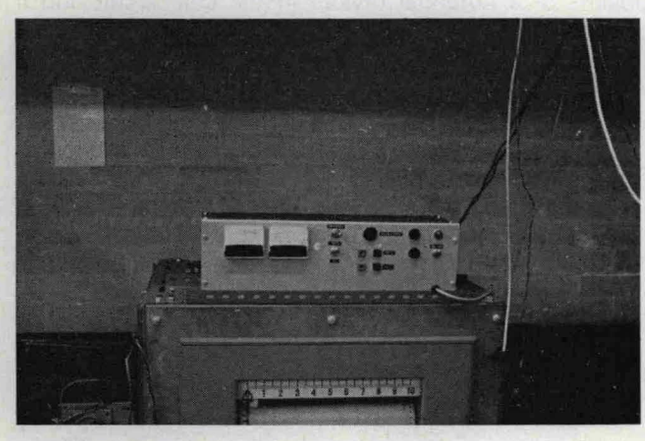

Fig. 4 Control unit (size, 17 in × 5 in × 5 in)

The coil controller may be constructed fairly cheaply, and uses only standard parts. While the simplicity of on–off control is an advantage, hunting may be a problem on low-viscosity liquids where damping is low. Hunting has, however, been eliminated in the present instrument by making use of a very low speed (1 rev/min) motor to drive the potentiometer; this motor is equipped with an electromagnetic brake to eliminate overshoot. Sensitivity may be varied by changing the mirror–photocell distance.

Acknowledgement

The authors wish to make acknowledgement to Professor Stacey G. Ward, Head of the Department of Minerals Engineering, for the provision of research facilities; to the Institution of Mining and Metallurgy for the provision of an equipment grant for the project on the viscosity of slags; and, particularly, to Mr. J. Mann, Department of Psychology, who designed the amplifier and constructed the coil controller, and who has given invaluable advice throughout the project.

References

1. **Bockris J. O'M. and Lowe D. C.** Viscosity and the structure of molten silicates. *Proc. R. Soc.*, **A226**, 1954, 423–35.
2. **Roberts D. A.** The measurement of the viscosity–temperature characteristics of copper smelting slags. Ph.D. thesis, University of Wales, 1959.
3. **Jones T. J. B.** Temperature–viscosity relationships of slags. Ph.D. thesis, University of Wales, 1962.
4. **Higgins R. and Jones T. J. B.** Viscosity characteristics of Rhodesian copper smelting slags. *Trans. Instn Min. Metall.*, **72**, Sept. 1963, 825–64.

A three-dimensional diagram for the silver–oxygen system

E. H. Baker Ph.D., D.I.C., F.R.I.C.
Research Fellow, Nuffield Research Group in Extraction Metallurgy, Imperial College, London
M. I. Talukdar M.Sc., Ph.D.
Nuffield Research Group in Extraction Metallurgy, Imperial College, London

53.072 : 541.123.2 : 546.57 : 546.21

The silver–oxygen system has been investigated at pressures of oxygen in the range 0·2–750 atmospheres.[1]

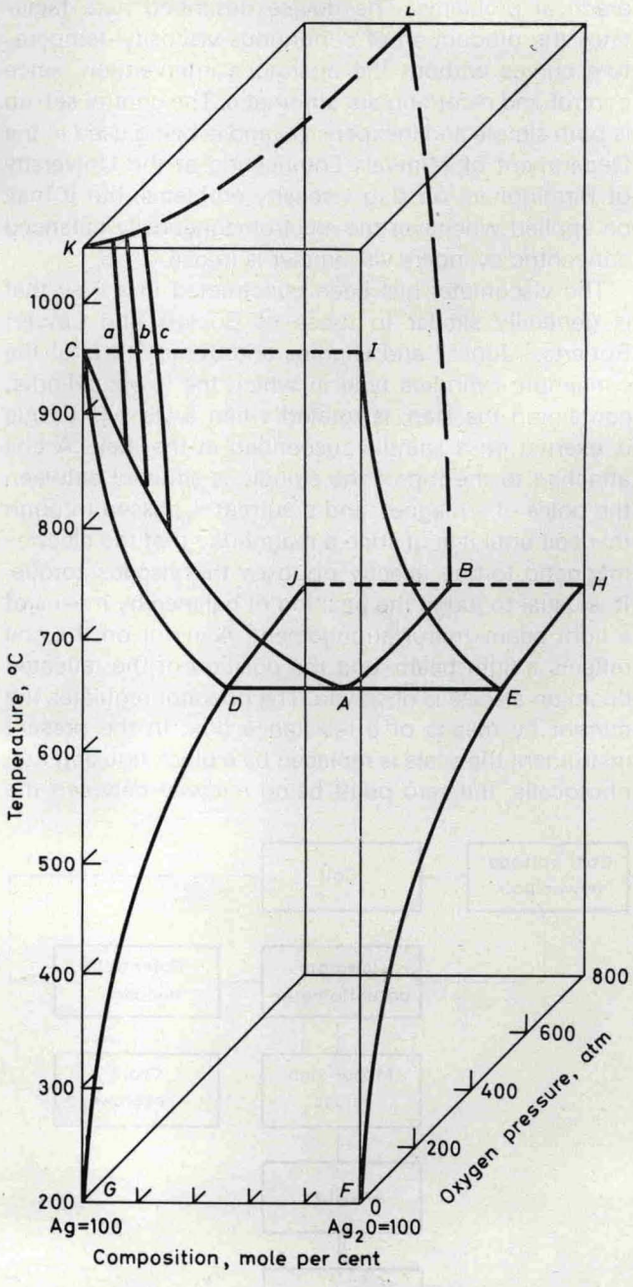

Fig. 1 Phase diagram for eutectic region of silver–oxygen system. Broken lines represent schematic portions

From thermogravimetric determinations the eutectic composition is found by extrapolation to be approximately Ag_2O 40 mole per cent, Ag 60 atom per cent; from these measurements a three-dimensional phase diagram has been constructed for the system (Fig. 1).

Cuprous oxide is structurally similar to silver oxide and behaves as a metal-deficit semiconductor;[2] silver oxide should therefore act likewise. No sub-oxide of silver, however, is formed[3] and no stable higher oxide appears to exist, so departures from stoichiometry of silver oxide should be small. Since the solubility of oxygen (or silver oxide) in solid silver is also small,[4] the solid phases in Fig. 1 are regarded as the normal oxide and pure silver.

Below the eutectic point (*A*) the equilibrium between the solid phases is independent of the amounts present and is represented by the unidirectionally parallel surface *DEFG*. The lines *AB* and *AC* give the compositions of melts in equilibrium with solid silver oxide and solid silver respectively; the projections of these lines—*EH* and *EI* (or *DJ* and *DC*)—represent the pressure–temperature relation for the melt region. The all-liquid region is represented by the surface *ACKLB*. At pressures up to 100 atm the shape of this surface is defined by means of the isobars *a*, *b* and *c*, obtained thermogravimetrically; at higher pressures the precise contours of the surface are uncertain.

With the carbonate systems[5,6] the pressures of carbon dioxide in equilibrium with the oxide phase and the melts increase with temperatures above the eutectic point, reaching a maximum before diminishing towards the melting point of the oxide. In contrast to this behaviour, the analogous equilibrium line here (*AC*) shows a continuous diminution of pressure from the eutectic point to the melting point of silver (961°C). The much larger temperature range involved with the carbonate systems will be a significant factor in this difference of equilibrium behaviour.

Allen heated a mixture of silver and silver oxide in a steel bomb, and obtained a micrograph of the cooled ingot which indicated eutectic melting.[7] In the present work, similar micrographs have been obtained from the cooled ingots of the binary melts formed by dissociation of the silver oxide above the eutectic point (i.e. melts lying along *AB*).[1] One of these from a melt at 548°C and 700 atm is shown in Fig. 2. Since the high-pressure furnace cooled rapidly, only the outer portions of the ingot reoxidized, and the section of the central portion depicted shows clearly the granular silver and the dark areas of the oxide.

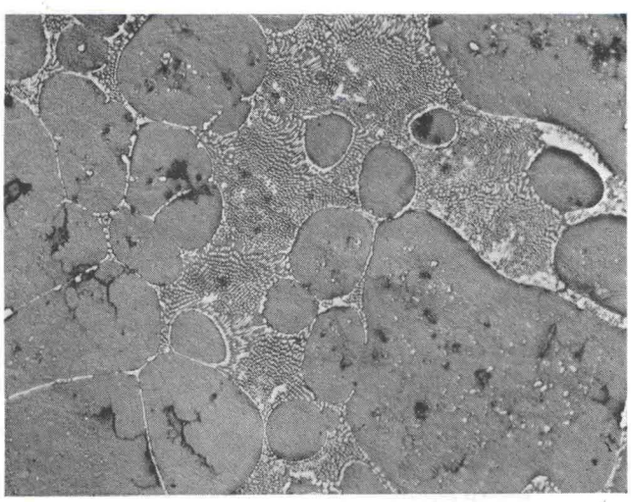

Fig. 2 Micrograph of solidified melt obtained at 548°C and 700 atm (unetched). Magnification, ×140

It is unlikely the melting point of silver oxide could be determined directly. Extrapolation of the line *AB* to 100 mole per cent Ag_2O indicates that the melting point of the silver oxide would be approximately 1000°C under a pressure of oxygen of at least 10^4 atm.

Acknowledgement

The authors thank the Science Research Council for financial support. One of them (M.I.T.) thanks the Association of Commonwealth Universities and the British Council for a scholarship.

References

1. **Baker E. H. and Talukdar M. I.** Silver–oxygen system in the pressure range 0·2–750 atm, and some measurements on silver–nitrogen and gold–oxygen equilibria. *Trans. Instn Min. Metall. (Sect. C: Mineral Process. Extr. Metall.)*, **77**, 1968, C128–33.
2. **Libowitz G. G.** Nonstoichiometry in chemical compounds. *Prog. solid-st. Chem.*, **2**, 1965, p. 241.
3. **Lewis G. N.** Concerning silver oxide and silver suboxide. *J. Am. chem. Soc.*, **28**, 1906, 139–58.
4. **Podgurski H. H. and Davis F. N.** The solubility of oxygen in silver and the thermodynamics of the internal oxidation of a silver–copper alloy. *Trans. Am. Inst. Min. Engrs*, **230**, 1964, 731–5.
5. **Baker E. H. and Butler J.** A phase diagram for the calcium oxide–carbon dioxide system in the eutectic region. *Nature, Lond.*, **195**, 1962, 173.
6. **Baker E. H.** A phase diagram for the barium oxide–carbon dioxide system in the eutectic region. *Nature, Lond.*, **206**, 1965, 1250–1.
7. **Allen N. P.** The effect of pressure on the liberation of gases from metals (with special reference to silver and oxygen). *J. Inst. Metals*, **49**, 1932, 317–46.

Phase equilibrium diagrams of the system $CaCl_2$–$CuCl$–$PbCl_2$

D. S. Coleman M.Sc., Ph.D., A.I.Ceram., A.M.I.Ref.Eng.
Lecturer in Materials Science, University of Technology, Loughborough, Leicestershire
P. D. A. Lacy B.Tech.
Metallurgy and Materials Section, Chemistry Department, University of Technology, Loughborough, Leicestershire

541.123.5 : 546.121.3 : 669.053

Extraction of low-grade ores and reclamation of scrap metals is often carried out using processes involving the chlorides of the metals concerned. Metals such as tin, copper and lead can be extracted by making use of the chlorides of these metals, which are collected for further refining. This method of extraction can involve the heating of the metal source material in a chlorine atmosphere to make the chloride; but, more often, it is made by heating with cheaper calcium chloride. Information on the phase relationships of the chlorides of metals is not readily available and the meagre amount of data on the chlorides of copper, calcium and lead which can be obtained has been collected by Levin *et al.*[1]

Previous researches by Coleman and Lacy[2] and Coleman and Spencer[3] have shown that systems containing chlorides or fluorides of metals can be determined readily with the hot-stage microscope technique. This technique has been shown to be reliable and accurate for determining binary and ternary systems; it is the method that has been used in this research.

Experimental details

Hot-stage microscope

The hot-stage microscope technique is well established and references to its development were reported in an earlier note[3] which explained how the technique has been adapted to measure temperatures of phase changes at liquidus, solidus and solvus boundaries. Details of the method of phase diagram determination will therefore not be reported here; the accuracy of temperature measurement in the technique is, however, estimated as ±3°C in the temperature range 0–1000°C.

For this particular research the hot-stage microscope cell was operated with an inert atmosphere obtained by passing dry nitrogen through the cell at a slow rate. This protected the materials during the determinations—from oxidation in the case of CuCl and $PbCl_2$ or deterioration of $CaCl_2$ due to moisture in the atmosphere.

Materials preparation

These were prepared by methods suggested by Brauer.[4]

Calcium chloride The anhydrous material was prepared from 'Analar' grade $CaCl_2 . 6H_2O$ by heating in a stream of dry hydrogen chloride gas for 3 hours at 100°C, followed by 1 h at 250°C and, finally, 1 h at 400°C.

Cuprous chloride 'Analar' grade $CuSO_4 . 5H_2O$ was dissolved in distilled water, sodium chloride was added and sulphur dioxide gas bubbled through the solution until white cuprous chloride was precipitated. It was filtered, washed with glacial acetic acid, ethanol and, finally, acetone while under an atmosphere of carbon dioxide gas. The precipitate was dried in warm air.

Lead chloride Dilute hydrochloric acid was added to a solution of 'Analar' grade lead nitrate. The precipitate was washed with cold distilled water and was dried in warm air.

All these materials were stored in a vacuum until required.

Mixture preparation

The correct amounts of materials were rapidly weighed into a platinum crucible. The mixture was heated in an atmosphere of dry nitrogen until molten, and the crucible was then allowed to cool rapidly. The mixture was quickly ground with a warm pestle and mortar before being stored under vacuum.

Results and discussion

Melting points of pure materials

The melting point of calcium chloride, as determined by the hot-stage microscope method, was 750°C. Menge[5] found a value of 777°C, but quoted references to values ranging between 719 and 806°C. Later references[6,7] gave the melting point as 772°C.

Cuprous chloride had a melting point of 425°C, which is in agreement with the values of other workers;[6–8] Menge, however, found cuprous chloride melting points ranging from 418 to 434°C.

The melting point of lead chloride was determined as 490°C, which is similar to the findings of Menge (496°C); Menge, however, quoted references to values ranging from 447 to 501°C.

Menge and Herrmann determined the melting points and phase diagram data by sealing samples in tubes with thermocouples embedded in them. Using a furnace with a controlled cooling rate, phase change data were obtained from cooling curves. Obviously, larger samples were used in these determinations in comparison with the hot-stage microscope method, but in the latter a greater number of determinations (usually more than a dozen for each value) is possible. Bearing in mind the difference in methods of determination, the agreement of results is good.

Binary phase equilibrium results

The phase equilibrium diagrams redetermined for the binary eutectic systems $CaCl_2$–$CuCl$ and $CaCl_2$–$PbCl_2$ are shown in Figs. 1 and 2 respectively. The binary